Per. Mineral. (2001), *70*, 1, 111-129 http://go.to/permin

PERIODICO di MINERALOGIA
established in 1930

An International Journal of
MINERALOGY, CRYSTALLOGRAPHY, GEOCHEMISTRY, ORE DEPOSITS, PETROLOGY, VOLCANOLOGY
and applied topics on *Environment, Archaeometry* and *Cultural Heritage*

Aluminium-phosphates and borosilicates in muscovite-kyanite metaquartzites near Diamantina (Minas Gerais, Brazil): Petrogenetic implications

GIULIO MORTEANI[1]* DIETRICH ACKERMAND[2] and ADOLF HEINRICH HORN[3]

[1] Lehrstuhl für Angewandte Mineralogie und Geochemie, Technische Universität München, Lichtenbergstrasse 4, 85747 Garching, Germany
[2] Institut für Geowissenschaften, Christian-Albrechts-Universität Kiel, Olshausenstrasse 40, 24105 Kiel, Germany
[3] Centro de Pesquisa Prof. Manuel Teixeira da Costa, Instituto de Geociências, Universidade Federal de Minas Gerais, Av. Antônio Carlos 6277, 31000 Belo Horizonte MG, Brazil

Submitted, November 2000 - Accepted, February 2001

ABSTRACT. — Within the muscovite-dumortierite-kyanite metaquartzites of the Middle Proterozoic Banderinha formation near Diamantina (State of Minas Gerais, Brazil), five rock types, A1 through A4, and B are distinguished on the basis of whole-rock composition. In addition to quartz, muscovite and Ti-bearing hematite (0.2 to 5.0 wt% TiO_2), the five rock types show the following typical mineral assemblages: A1: lazulite, kyanite, andalusite; A2: lazulite, kyanite, augelite; A3: lazulite, amblygonite, berlinite, tourmaline; A4: lazulite, goyazite, tourmaline, kyanite, and B: dumortierite, kyanite. From lithostratigraphical considerations, microscopic investigations and microprobe mineral analyses, as well as stable oxygen isotope thermometry, these parageneses formed at a maximum temperature of 440°C and pressure of at least 3.4 kbar during the multistage Brasiliano tectonothermal episode between 680 and 450 Ma. Considerable solid solution series exist between lazulite and scorzalite (Mg ⇔ Fe), goyazite and svanbergite (P ⇔ S) and goyazite and crandallite (Sr ⇔ Ca). The MgO/FeO ratio of lazulite increases with the increasing MgO/FeO ratio of the bulk rock. A contact between lazulite and dumortierite was never observed. The protolith of the lazulite-bearing layer was probably a phosphorus- and locally also boron-rich clay-bearing sandstone deposited in a sabkha-like environment in originally highly alkaline conditions. In the study area, the lazulite-bearing muscovite-kyanite metaquartzites mark the strongly tectonised contact between the Middle Proterozoic Rio Paraúna and Espinhaço supergroups.

* Corresponding author, E-mail: da@min.uni-kiel.de

RIASSUNTO. — Sulla base della loro composizione chimica le metaquarziti a muscovite, dumortierite e cianite che si trovano presso Diamantina nello stato di Minas Gerais (Brasile) possono essere riferite ai tipi A1, A2, A3, A4 e B. In aggiunta a quarzo, muscovite ed ematite titanifera (0,2 fino a 5,0 % in peso di TiO_2) i cinque tipi di roccia si differenziano nell'associazione mineralogica come segue: A1: lazulite, cianite, andalusite; A2: lazulite, cianite, augelite; A3: lazulite, ambligonite, berlinite, tormalina; A4: lazulite, goyazite, tormalina, cianite; B: dumortierite, cianite. Le metaquarziti fanno parte della formazione detta Banderinha. Da considerazioni di litostratigrafia, osservazioni al microscopio, e termometria basata sugli isotopi dell'ossigeno, tali associazioni mineralogiche si formarono durante l'evento tettonotermico Brasiliano posto fra 680 ed 450 Ma ad una temperatura attorno ai 440°C ed una pressione di almeno 3,4 kbar. Lo studio alla microsonda mostra che esiste una notevole soluzione solida fra lazulite e scorzalite (Mg ⇔ Fe), fra goyazite e svanbergite (P ⇔ S) e goyazite e cranadallite (Sr ⇔ Ca). Nella lazulite il rapporto MgO/FeO aumenta con

l'aumento dello stesso rapporto nella roccia totale. Non è stata trovata una paragenesi di contatto fra lazulite e dumortierite. Nella zona studiata, le metaquarziti a lazulite e dumortierite sono presenti al contatto, fortemente tettonizzato, fra i supergruppi medio proterozoici Rio Parauna ed Espinhaço. Il protolito delle metaquarziti può essere considerato una arenaria con componente argillosa ricca in fosforo e boro, e l'ambiente di deposizione si può supporre una *sabkha* altamente alcalina.

KEY WORDS: *Amblygonite, andalusite, augelite, berlinite, Brazil, crandallite, dumortierite, goyazite, kyanite, lazulite, Proterozoic, metaquartzite, scorzalite, svanbergite.*

INTRODUCTION

Information about the occurrences of phosphate minerals, other than apatite, in metamorphic rocks and their P-T stability is rarely found in the literature. Little information exists regarding phase relations in rocks containing both aluminium phosphates and aluminium borosilicates such as dumortierite. In Brazil, lazulite-bearing rocks are mentioned from Minas Gerais (Cassedanne and Cassedanne, 1975) and Bahia (Bank, 1972; Eberle, 1972; Cassedanne *et al.*, 1989; Cassedanne, 1990). The occurrence of dumortierite with lazulite in Brazil is described by Cassedanne and Franco (1966) and Cassedanne *et al.* (1989) only from the Serra de Vereda in Bahia. In all cases, a detailed petrological description including whole-rock and mineral geochemistry is missing.

The aim of the present paper is to present a petrological description including whole-rock and mineral chemistry, trace element composition, and textural relations of phosphates lazulite, augelite, amblygonite, goyazite and of borosilicates dumortierite and tourmaline in the muscovite-kyanite metaquartzites found within the upper Archean Banderinha formation in the area of Diamantina (State of Minas Gerais, Brazil) and to discuss on the basis of those data the P,T conditions of the metamorphic overprint and the depositional environment of the protolith of the metaquartzites.

The rocks studied in this paper are examples of the rather rare cases of sedimentary phosphate-rich rocks of Middle Proterozoic age.

GEOLOGICAL SETTING

The lithological sequence, corresponding ages and structural relations in the studied area are still under discussion, *e.g.* by Pflug (1968), Dorr (1969), Schöll and Fogaça (1979; 1981), Fogaça and Schöll (1984), Almeida Abreu *et al.* (1992), Dussin (1994), Almeida Abreu (1994, 1996), Silva (1995) and Horn *et al.* (1996).

As shown in fig. 1, the sequence starts in the study area with the Archean Basal Complex formed of the Gouveia group, *i.e.* a series of granitic to granodioritic gneisses, amphibolites and migmatites. In the study area, the Basal Complex is overlain discordantly by the Middle Proterozoic Rio Paraúna supergroup and the Costa Sena group, and is considered by Pflug and Carvalho (1964), Pflug (1965), Herrgesell and Pflug (1986), Pflug *et al.* (1980) and Almeida Abreu (1994) as the remnant of a greenstone belt. The Costa Sena group is subdivided into a lower and upper Barão de Guacuí formation and the uppermost Banderinha formation (Pflug, 1968; Fogaça and Schöll, 1984). However, according to Almeida Abreu (1994, 1996), Silva (1995) and Horn *et al.* (1996), the Banderinha formation is the basal part of the Guinda group and therefore the lowermost formation of the Espinhaço supergroup, which is found lying with an erosive contact discordantly on top of the Barão de Guacuí formation. Within the Guinda group, the Banderinha formation is overlain by the São João de Chapada, Sopa Brumadinho and Galho do Miguel formations.

According to Almeida Abreu (1996), the lithology of the Banderinha formation consists of micaceous meta-arenites and subordinate metaconglomerates and metapelites. The phosphates and borates occur in the lowermost part. Lazulite occurs predominantly in a mostly

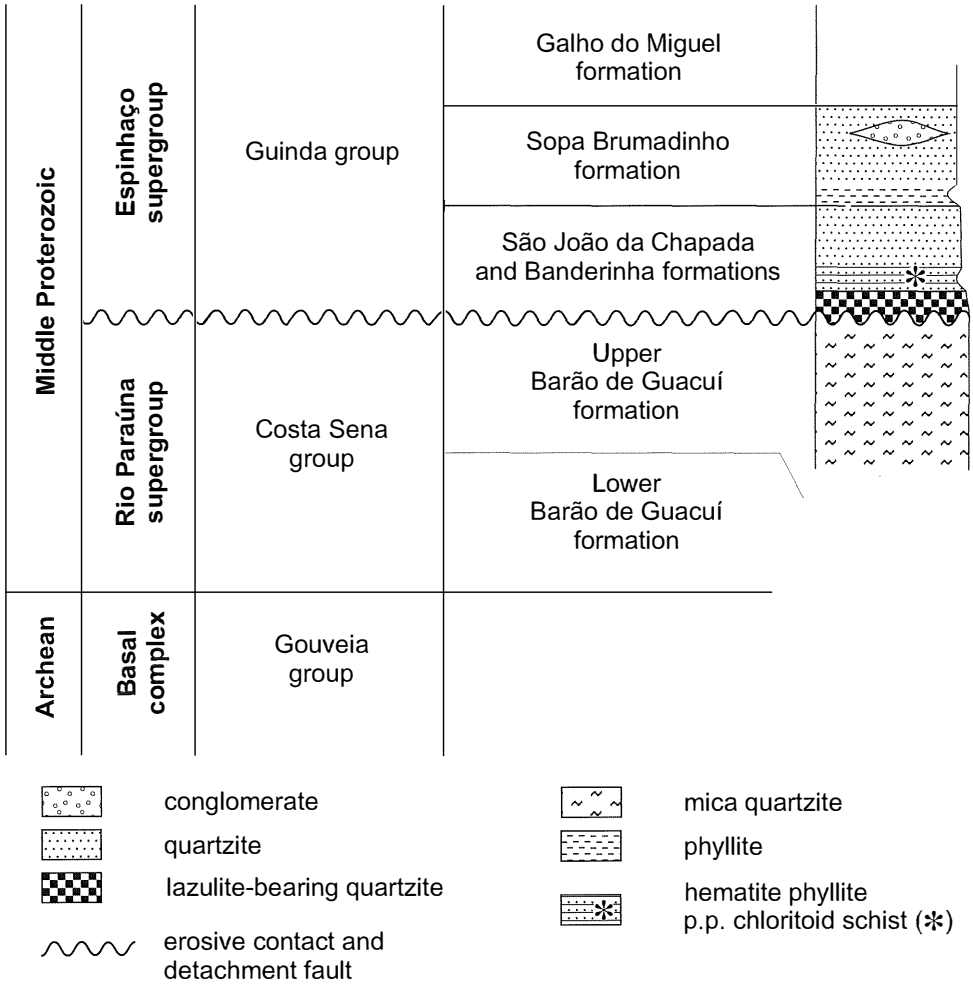

Fig. 1 – Lithostratigraphic column of rock units in area of Diamantina in Serra do Espinhaço (State of Minas Gerais, Brazil) according to Schöll and Fogaça (1979, 1981), Almeida Abreu (1994, 1996) and Horn *et al.* (1996). Lazulite-bearing strata are found in lowermost part of Banderinha formation at contact with overlying Barão de Guacuí formation.

soft muscovite-kyanite metaquartzite, as homogeneously distributed small (1 to 3 mm) pale blue grains. Individual lazulite grains or aggregates with the typical deep blue colour are quite rare.

Rarely lazulite is enriched in foliation planes and as rounded anhedral crystals up to 2 - 3 cm in diameter in quartz-hematite/ilmenite veins discordantly cutting the schistosity. Dumortierite occurs rarely as very small bright blue needles in muscovite-rich layers of the metaquartzite. Outcrops with lazulite-bearing metaquartzites are quite rare, so that sampling was limited to a few localities.

A geological sketch-map of the study area, based on the lithostratigraphic column given in fig. 1, the map given in Schöll and Fogaça (1981) and our own mapping results, is presented in fig. 2, together with the sampling points. Because of the Middle Proterozoic age

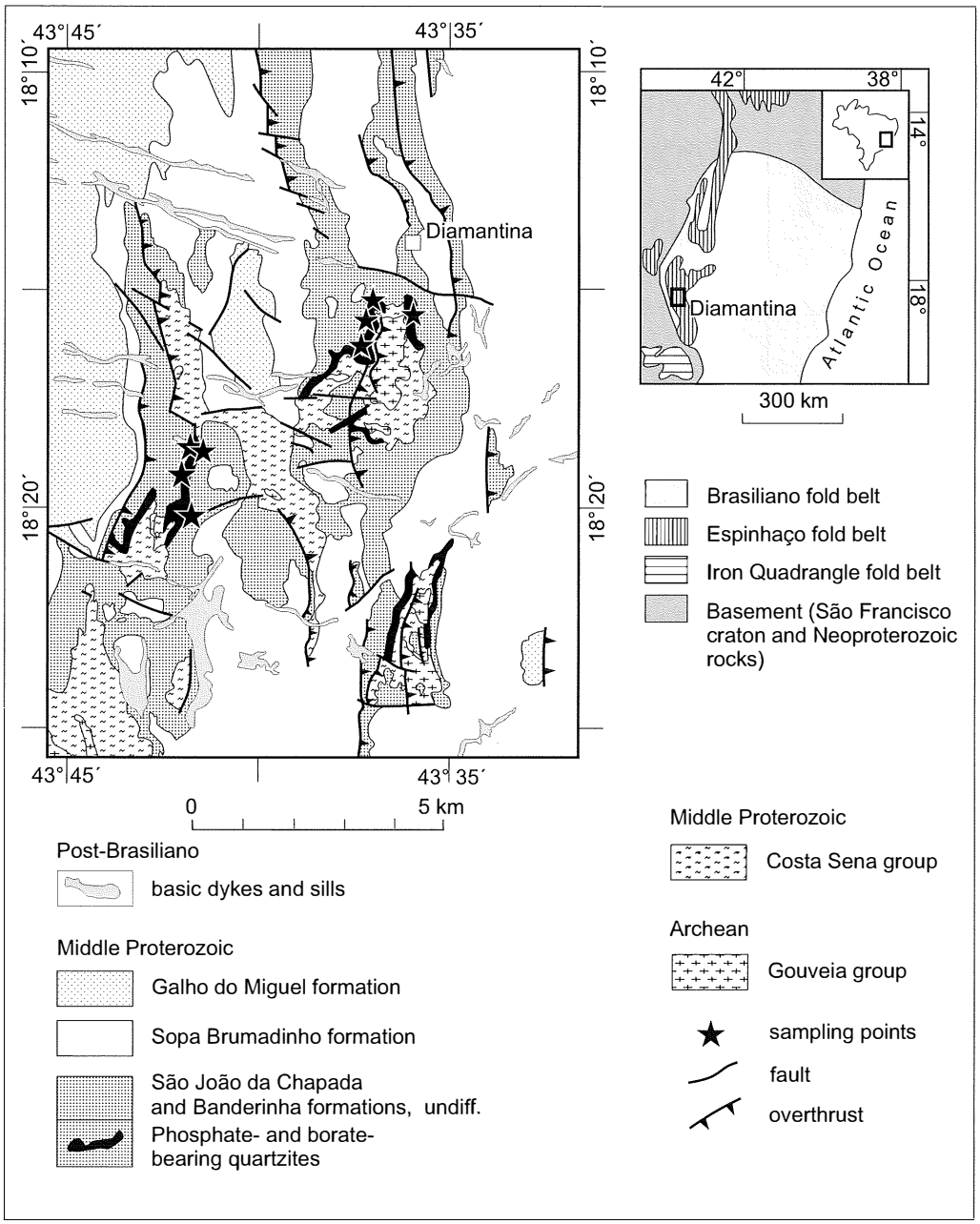

Fig. 2 – Simplified geological sketch map of Diamantina area according to Schöll and Fogaça (1981) and own mapping results, showing distribution of lazulite-bearing Banderinha formation and sampling points.

of the protolith, of at least 1750 to 1710 Ma, the Banderinha formation (Almeida Abreu, 1996) may have undergone not only the Rondoniano/Espinhaço (1200 Ma) but also the Brasiliano (680 - 450 Ma) tectonometamorphic events (Söllner *et al.,* 1991; Almeida Abreu, 1994; Dussin, 1994).

Analytical methods

Whole-rock REE, Ta, Sc, Zr, Hf, Cs, U and Th contents were determined by standard INAA, Li by AAS, FeO by colorimetry, and B by ICP-OES. All other major and trace elements were analysed by a fully automated Siemens XRF using Li-tetraborate glass disks.

Microprobe analyses of the minerals were obtained with a Cameca «Camebax Microbeam» electron-microprobe with four wavelength-dispersive spectrometers and an online PaP-correction program (Pouchou and Pichoir, 1984), using fluorapatite (Ca, P, F, Cl), wollastonite (Ca, Si), synthetic corundum (Al), synthetic periclase (Mg), Fe-metal (Fe), synthetic $SrCuSi_4O_{10}$ (Sr) and pyrite (S) for major elements. Various glass standards were used to determine trace elements. Operating conditions were 15 kV accelerating voltage and 15 nA beam current, which allows a beam smaller than 0.5 micrometres. For the analysis of all phosphates, a defocussed beam with a diameter of 2 micrometres was used, because time-dependent measurements indicated a count rate loss for several elements when a highly focussed beam was used.

The oxygen isotope composition of quartz and hematite was measured on a Finnigan Mat 251 spectrometer. Oxygen was extracted from the mineral by reaction with BrF_5 and converted to CO_2 over hot graphite according to Clayton and Mayeda (1963). Oxygen isotope composition was measured on a Finnigan MAT 251 mass spectrometer and reported as δ values relative to V-SMOW in per mil (‰). Analytical reproducibility was within 0.2%. The equilibrium isotope temperature between quartz and hematite of 440°C results from the equation given by Zheng and Simon (1991). The shaded temperature interval given in fig. 7 encompasses the temperature range that results from the use of other equilibrium data (e.g. Bottinga and Javoy, 1973; Chiba *et al.*, 1989).

Whole-rock chemistry

On the basis of whole-rock chemistry and mineral assemblages (see below), the muscovite-kyanite metaquartzites can be subdivided into lazulite-bearing rock types A1 through A4, and dumortierite-bearing rocks, type B.

Major element compositions and discriminating trace elements are listed in Table 1 for selected samples of the five rock types.

Table 1 shows that the P_2O_5/Al_2O_3 ratio increases from rock type B to A4, A3, A2 and A1. Trace element contents of the rock types are also very different: type A4 has the highest Sr, Zr and Nb contents as compared to all other types.

Fig. 3 shows the NASC (North American Shale Composite; McLennan, 1989) normalised whole-rock REE distribution patterns of the various rock types. They all show typical pattern of sediments but, in comparison to NASC, higher LREE contents and slightly lower HREE contents. The scatter in the LREE is much more marked than in the HREE. Monazite, xenotime and zircon are the main carriers of REE in metaquartzites. Monazite preferentially incorporates LREE. It may therefore be presumed that the LREE scatter is due to different amounts of accessory monazite in the analysed metaquartzites.

Petrography and mineral chemistry

Microscopical investigations revealed the following assemblages in addition to quartz, muscovite and Ti-bearing hematite:

rock type A1: lazulite, (lazulite-muscovite-quartz symplectite), andalusite, kyanite.

TABLE 1

Representative bulk analyses of rock types A1 to A4 and B.

Rock-type	A1		A2			A3				A4			B
sample	5726	5727	5711	5712	5708	5714	5717	5715	5716	5722	5723	5725
SiO_2 [wt%]	62.28	64.60	74.16	73.90	63.70	63.80	64.80	68.30	69.11	55.90	76.70	76.10
TiO_2	0.07	0.08	0.15	0.13	0.07	0.09	0.10	0.25	0.34	0.50	0.76	0.31
Al_2O_3	16.99	16.80	13.23	12.88	21.70	21.00	21.20	16.10	17.31	27.10	14.00	17.70
Fe_2O_3*	1.84	2.42	1.74	1.69	2.04	2.38	1.93	3.47	2.81	2.79	1.30	2.38
MgO	2.41	1.32	0.77	0.71	0.44	0.70	0.52	0.70	0.27	0.48	0.05	-
CaO	0.19	0.14	-	-	0.03	0.02	0.02	0.02	-	0.04	0.02	0.02
Na_2O	0.14	0.05	0.05	0.07	0.28	0.14	0.14	0.06	0.09	0.33	0.01	n.a.
K_2O	1.79	1.70	1.90	1.54	5.86	5.38	5.69	3.48	4.59	6.86	3.49	1.13
P_2O_5	11.69	9.67	4.71	5.44	1.42	3.55	2.23	4.64	1.35	0.46	0.29	0.04
F	0.23	n.a.	0.26	0.16	n.a.	n.a.	n.a.	n.a.	0.23	n.a.	n.a.	n.a.
S	-	-	0.01	0.02	-	0.04	0.02	-	0.14	0.08	-	0.14
LOI	3.5	3.5	1.8	2.0	2.7	2.6	2.7	2.8	2.8	3.5	1.8	0.7
total	101.63	101.28	98.78	98.54	98.24	99.70	99.35	99.82	99.04	98.04	98.42	98.57
B [ppm]	18	n.a.	24	n.a.	n.a.	477	473	14	85	2670	n.a.	25
Ba	461	263	62	63	165	153	160	339	163	167	64	64
Nb	-	8	17	17	12	-	12	23	30	37	46	27
Ni	54	50	31	34	30	40	34	57	16	39	14	12
Rb	52	63	43	39	175	149	161	88	113	161	96	40
Sr	1646	1048	1132	969	338	476	364	4889	4296	2937	1669	75
V	11	-	-	16	6	-	-	25	23	72	94	30
Y	75	60	37	28	15	43	37	54	47	41	44	21
Zr	51	46	103	56	-	-	20	116	189	293	87	218
MgO/FeO**	1.45	0.61	0.49	0.47	0.24	0.33	0.43	0.22	0.11	0.19	0.04	-

-: below detection limit; n.a.: not analysed; *: total Fe calculated as Fe_2O_3 (** total Fe calculated as FeO)
As below detection limit, in 5726 As= 67 ppm.

rock type A2: lazulite, (lazulite-muscovite symplectite), augelite, kyanite.

rock type A3: lazulite, amblygonite, tourmaline, berlinite.

rock type A4: lazulite, goyazite, (lazulite rimmed by goyazite), kyanite, tourmaline.

rock type B: dumortierite, kyanite.

Representative microprobe analyses of the silicate, phosphate and borosilicate minerals are given in Tables 2*a*, 2*b* and 3.

Microscopical investigations showed that, in rock type A1, lazulite occurs as small anhedral grains, often as clusters included in large anhedral andalusite grains. In rock type A2, lazulite occurs mainly as a rim around patches of augelite, partially replaced by fine-grained muscovite-quartz symplectite (fig. 4*a*). In rock type A3, lazulite is found as large blue anhedral grains with inclusions of muscovite, quartz, amblygonite and euhedral tourmaline. In rock type A4, lazulite occurs as typical polycrystalline and quite fine-grained patches, surrounded by brownish goyazite-svanbergite-muscovite symplectite (fig. 4*b*).

Very fine-grained hematite, typically found in the cores of large lazulite grains of rock type A3, demonstrates that lazulite started to crystallize at a very early stage of the history of the rock, when it still had the fine-grained but already folded texture of unmetamorphosed, or at most very low grade metamorphosed, pelitic sediment. Sigmoidal internal structures,

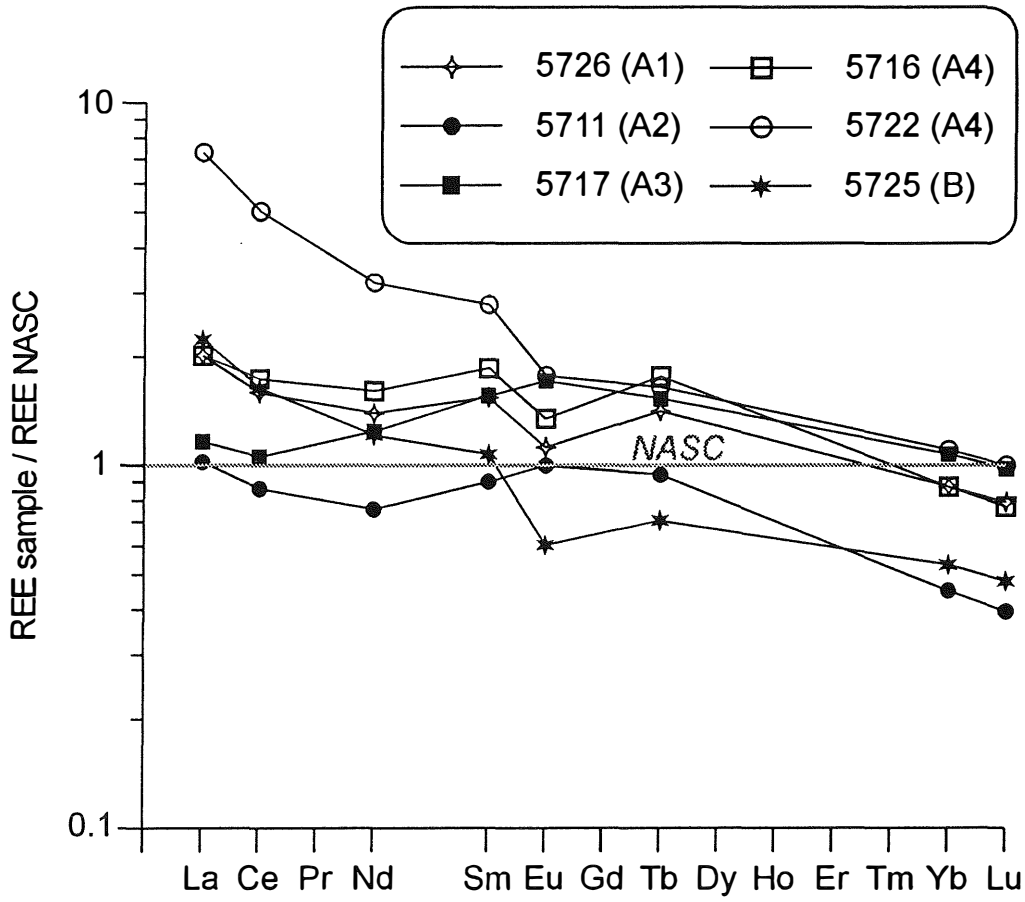

Fig. 3 – NASC-normalised whole-rock REE distribution patterns of various rock types.

marked by coarse-grained hematite, demonstrate that the lazulite rim was formed during tectonic deformation, connected with increasing metamorphism and a coarsening of the grain size of hematite. Changing P,T conditions during metamorphism are also revealed by colour zoning of lazulite, with light blue cores and dark blue rims.

The chemical composition of lazulite follows the theoretical formula $(Mg,Fe)Al_2(PO_4)_2(OH)_2$ (Table 2*a*). Fig. 5*a* shows the Mg *vs* Fe contents of lazulite from rock types A1 to A4. The composition plots very close to the substitution line of Fe for Mg, thus indicating a very low Fe^{3+} content.

Fig. 5*b*, in which the MgO/FeO ratio of lazulite vs. the whole-rock MgO/FeO ratio is plotted shows that the lazulite MgO/FeO ratio depends on that of the whole-rock.

Lazulite in rock types A2, A3 and, partly, A4, shows enhanced F contents with respect to the lazulite of rock type A1 (Table 2a). This indicates the possible substitution of OH by F in the formula, although such a substitution is not considered in the general formula given by Mandarino (1999).

TABLE 2*a*

Representative microprobe analyses and mineral formulas of Al-phosphate minerals found in rock types A1 to A4.

	lazulite-scorzalite (ss)									augelite		amblygonite			svanbergite-goyazite (ss)			
rock-type	A1		A2	A3				A4		A2		A3			A4			
sample	5726	5726	5711	5708	5708	5717	5717	5716	5722	5711	5711	5708	5717	5717	5716	5716	5722	5722
description	rim	core	(small)	rim	core	rim	core	(large)	(large)						(large)	(large)	(small)	(small)
SiO_2	0.20	0.22	0.66	0.36	0.04	0.64	0.06	0.16	0.08	0.25	0.17	-	0.04	0.60	0.21	0.27	0.21	0.33
TiO_2	0.03	-	-	0.11	0.06	-	-	0.04	0.08	0.03	-	-	-	-	-	-	0.03	0.05
Al_2O_3	32.75	33.15	32.99	31.90	32.47	31.39	32.13	31.09	31.10	46.91	48.70	25.91	34.95	31.42	31.51	30.77	35.20	33.90
Fe_2O_3*	-	-	-	-	-	-	-	-	-	1.50	0.20	10.97	1.21	2.37	-	-	-	-
FeO*	0.53	0.47	3.51	4.53	4.79	4.76	4.58	7.49	7.97	-	-	-	-	-	0.77	0.84	1.01	0.69
MgO	13.67	13.94	11.47	10.99	10.78	11.35	10.45	9.30	9.22	0.07	0.04	-	-	-	0.01	0.01	0.07	0.04
CaO	0.01	-	0.02	0.01	0.01	0.01	-	0.01	-	0.01	0.01	0.34	-	0.39	0.22	0.35	6.88	5.19
SrO	-	0.03	-	-	-	-	-	-	-	-	-	-	-	-	21.55	21.12	11.12	13.54
Na_2O	-	-	-	-	-	-	0.02	-	-	-	-	-	0.01	-	0.02	-	-	0.01
K_2O	0.02	0.01	0.10	0.02	-	-	-	0.02	0.02	0.03	0.03	-	0.01	0.17	0.04	0.06	0.01	0.04
P_2O_5	49.59	49.46	47.74	47.62	46.41	46.08	48.10	45.91	46.74	36.40	36.19	48.38	51.27	49.27	20.04	21.05	32.51	31.91
SO_3	-	-	-	-	-	-	-	-	-	0.05	-	-	0.01	0.04	12.98	11.45	2.58	0.42
As_2O_3	-	-	0.22	0.11	0.05	0.17	0.94	-	-	0.29	0.30	-	-	0.12	-	-	-	-
F	0.09	0.35	2.12	2.76	2.33	2.28	2.03	2.41	0.08	1.92	1.94	-	2.66	2.37	-	-	-	-
**anhydrous total	96.85	97.48	97.96	97.30	95.96	95.72	97.46	95.42	95.26	86.65	86.76	85.60	89.04	85.75	87.35	85.82	89.62	86.12
cations					P=4					P=4			P=4				P+S=4	
Si	0.02	0.02	0.07	0.04	-	0.07	0.01	0.02	0.01	0.03	0.02	-	-	0.06	0.04	0.05	0.03	0.05
Ti	-	-	-	0.01	0.01	-	-	-	-	-	-	-	-	-	-	-	-	0.01
Al	3.68	3.73	3.85	3.73	3.90	3.79	3.72	3.77	3.71	7.18	7.49	2.98	3.80	3.55	6.21	6.05	5.74	5.87
Fe^{3+}	-	-	-	-	-	-	-	-	-	0.15	0.02	0.81	0.08	0.17	-	-	-	-
Fe^{2+}	0.04	0.04	0.29	0.38	0.41	0.41	0.38	0.65	0.67	-	-	-	-	-	0.11	0.12	0.12	0.09
Mg	1.94	1.99	1.69	1.62	1.64	1.74	1.53	1.43	1.39	0.01	0.01	-	-	-	-	-	0.02	0.01
Ca	-	-	-	-	-	-	-	-	-	-	-	0.04	-	0.04	0.04	0.06	1.02	0.82
Sr	-	-	-	-	-	-	-	-	-	-	-	-	-	-	2.09	2.12	0.89	1.15
Na	-	-	-	-	-	-	-	-	-	-	-	-	-	-	0.01	-	-	-
K	-	-	0.01	-	-	-	-	-	-	0.01	0.01	-	-	0.02	0.01	0.01	-	0.01
P	4.00	4.00	4.00	4.00	4.00	4.00	4.00	4.00	4.00	4.00	4.00	4.00	4.00	4.00	2.84	2.98	3.81	3.97
S	-	-	-	-	-	-	-	-	-	-	-	-	-	-	1.16	1.02	0.19	0.03
As	-	-	0.01	0.01	-	0.01	0.06	-	-	0.02	0.02	-	-	-	-	-	-	-
F	0.03	0.11	0.66	0.87	0.75	0.74	0.63	0.78	0.03	0.79	0.81	-	0.78	0.72	-	-	-	-

*: Fe calculated as FeO or Fe_2O_3; **: anhydrous total with F≡O; (ss): solid solution; (small, large): grain size; -: below detection limit or not analysed. La_2O_3 in svanbergite - goyazite (ss) 0.02 wt%, Ce_2O_3 0.10 wt%.

TABLE 2*b*

Representative microprobe analyses and mineral formulas of silicate minerals found in rock types A1 to A4.

	muscovite							kyanite	tourmaline				
rock-type	A1	A2	A3				A4	A1	A3			A4	
sample	5726	5711+	5708+	5708	5717+	5717	5722	5726	5708	5708	5717	5716	5722
SiO_2	50.53	49.99	51.83	49.42	49.62	45.40	49.80	37.94	36.73	37.40	37.13	37.66	38.00
TiO_2	-	0.08	0.01	0.11	0.16	-	0.07	0.05	0.19	0.35	0.19	0.02	0.09
Al_2O_3	38.00	37.81	37.21	36.73	36.04	34.28	37.02	62.84	32.28	33.18	33.56	35.91	33.13
Fe_2O_3**	-	-	-	-	-	-	-	0.37	-	-	-	-	-
FeO**	1.28	1.80	2.51	2.17	2.49	2.21	2.41	-	12.26	10.74	10.63	3.28	8.09
MgO	0.09	0.05	0.16	0.11	0.14	0.13	0.18	-	3.07	3.63	3.60	6.65	5.94
CaO	-	0.03	0.02	0.01	0.02	-	-	-	0.02	0.01	-	-	0.01
Na_2O	0.20	0.23	0.20	0.25	0.23	0.27	0.12	-	1.20	1.15	1.18	1.01	1.81
K_2O	7.54	6.07	5.01	9.53	5.99	9.73	6.71	0.01	0.05	0.03	0.03	0.04	0.06
P_2O_5	0.20	0.03	0.02	-	0.03	0.05	0.02	0.01	0.04	-	-	0.32	0.01
SO_3	-	-	0.02	-	0.03	-	-	0.01	-	-	-	-	-
F	-	0.45	0.04	-	-	-	-	-	-	0.02	0.04	-	-
anhydrous total	97.87	96.35	97.01	98.33	94.75	92.07	96.33	101.23	85.84*	86.50*	86.34*	84.89*	87.14*
oxygens/ formula unit	22	22	22	22	22	22	22	10	24.50	24.50	24.50	24.50	24.50
Si	6.36	6.36	6.50	6.31	6.43	6.24	6.37	2.02	6.12	6.12	6.08	6.02	6.11
Ti	-	0.01	-	0.01	0.02	-	0.01	-	0.02	0.04	0.02	-	0.01
Al	5.63	5.65	5.50	5.53	5.50	5.55	5.58	3.95	6.34	6.40	6.48	6.77	6.28
Fe^{3+}	-	-	-	-	-	-	-	0.01	-	-	-	-	-
Fe^{2+}	0.13	0.19	0.26	0.23	0.27	0.25	0.26	-	1.71	1.47	1.46	0.44	1.09
Mg	0.02	0.01	0.03	0.02	0.03	0.03	0.03	-	0.76	0.89	0.88	1.59	1.42
Ca	-	-	-	-	-	-	-	-	-	-	-	-	-
Na	0.05	0.06	0.05	0.06	0.06	0.07	0.03	-	0.39	0.37	0.37	0.31	0.56
K	1.21	0.98	0.80	1.55	0.99	1.71	1.10	-	0.01	0.01	0.01	0.01	0.01
P	0.02	-	-	-	-	0.01	-	-	0.01	-	-	0.04	-
S	-	-	-	-	-	-	-	-	-	-	-	-	-
F	-	0.18	0.02	-	-	-	-	-	-	0.01	0.02	-	-

**: Fe calculated as FeO or Fe_2O_3; -: below detection limit or not analysed. *: anhydrous total without B_2O_3. + : fine-grained.

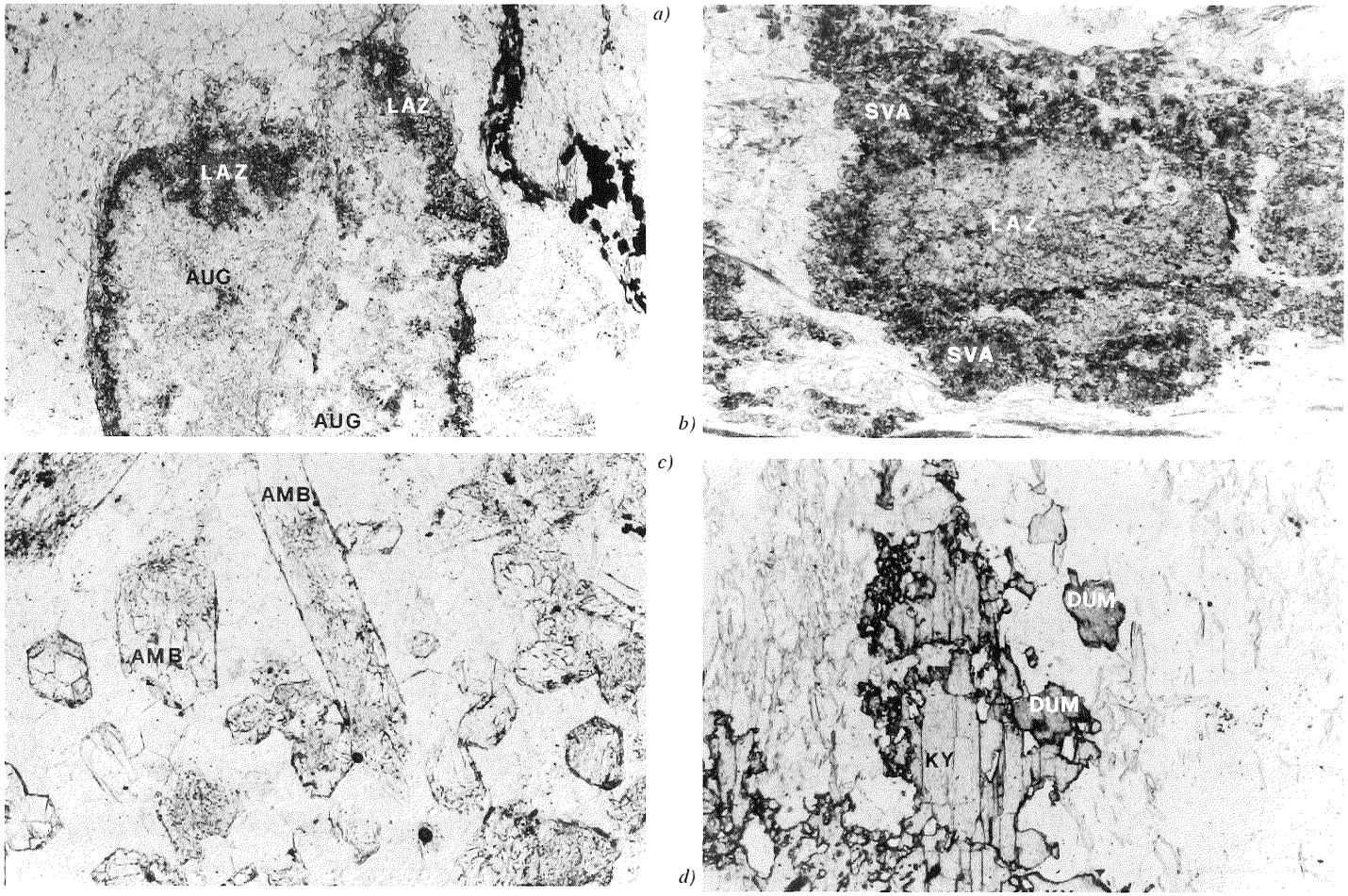

Fig. 4 – Microphotographs of: *a)* Relics of augelite (Aug) set in fine-grained muscovite-quartz symplectite rimmed by fine-grained lazulite (Laz); *b)* Anhedral aggregate of fine-grained lazulite (Laz) surrounded by svanbergite (Sva) rim. Svanbergite forming inner part of rim is poorer in sulphur, with respect to that forming outer part of rim; *c)* Subhedral amblygonite group crystals (Ambl), showing cloudy brownish staining. Microprobe analysis reveals increased Fe content; *d)* Dumortierite (Dum) included in rim of kyanite and quartz-muscovite matrix.

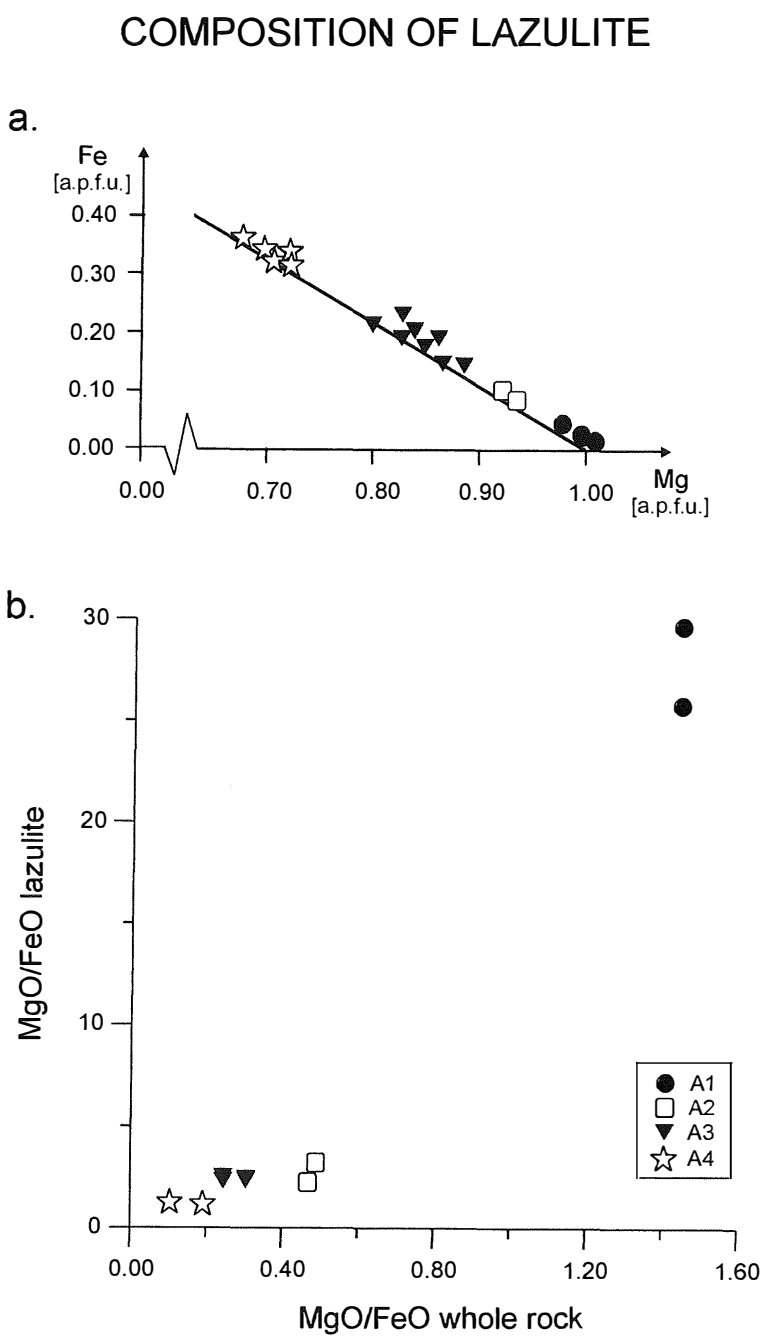

Fig. 5 – *a)* Plot of Mg *vs* Fe (a.p.f.u.) for lazulite of rock types A1 to A4. Solid line ideal Mg ⇔ Fe substitution; *b)* Plot of whole-rock *vs* lazulite MgO/FeO ratio. MgO/FeO ratio in lazulite increases with increasing whole-rock ratio.

TABLE 3

Representative microprobe analyses and mineral formulas of silicate and borosilicate minerals found in rock type B.

	muscovite		kyanite	dumortierite	
SiO_2	49.39	49.73	37.31	31.03	31.11
TiO_2	0.09	0.05	0.02	0.80	0.71
Al_2O_3	36.43	37.76	61.29	60.04	59.89
Fe_2O_3*	-	-	0.47	0.39	0.34
FeO*	1.87	1.57	-	-	-
MgO	0.02	0.06	-	0.58	0.57
CaO	0.03	0.02	0.01	-	0.02
Na_2O	0.22	0.18	0.02	-	-
K_2O	8.95	6.59	0.02	0.02	0.01
P_2O_5	0.03	0.03	0.04	0.04	0.10
F	-	-	0.17	-	-
total	97.03**	95.99**	99.28	92.90***	92.75***
oxygens/					
formula unit	22	22	10	33	33
Si	6.35	6.35	2.03	5.99	6.01
Ti	0.01	-	-	0.12	0.10
Al	5.52	5.68	3.93	13.67	13.65
Fe^{3+}	-	-	0.02	0.06	0.05
Fe^{2+}	0.20	0.17	-	-	-
Mg	-	0.01	-	0.17	0.16
Ca	-	-	-	-	-
Na	0.05	0.04	-	-	-
K	1.47	1.07	-	-	-
P	-	-	-	0.01	0.02
F	-	-	0.03	-	-

*: Fe calculated as FeO or Fe_2O_3; **: anhydrous total; ***: total without boron-oxide; -: below detection limit (~0.01); SO_3 in dumortierite 0.01 - 0.04 wt%.

Augelite occurs as colourless anhedral grains with a low refraction index and yellowish interference colour in polycrystalline clusters, mostly included in a muscovite-quartz symplectite usually rimed by fine-grained lazulite (fig. 4*a*). Augelite may form up to 10 vol% of rock type A2.

The chemical composition of augelite is given in Table 2a. It deviates only slightly from the ideal composition $Al_2(PO_4)(OH)_3$, due to Fe_2O_3 and As_2O_3 contents up to 1.5 and 0.3 wt%, respectively, which indicate substitutions of Al^{3+} and P^{5+} by Fe^{3+} and As^{5+}.

Amblygonite group minerals occur in rock type A3 as euhedral prismatic grains in coarse-grained veinlets or patches of mobilised quartz and disseminated as anhedral grains associated with kyanite and lazulite. These minerals show typical patchy brownish staining (fig. 4*c*).

The general formula of amblygonite group minerals is $AB(PO_4)X$, in which A = Li, Na; B = Al, Fe^{3+} and X = OH, F. The amblygonite group minerals analysed here show a quite inhomogeneous patchy composition. Typical examples are listed in Table 2a. The colourless sample 5717 (Table 2*a*), due to the low Fe

content (1.21 wt%), has a composition close to that of montebrasite $LiAl(PO_4)(F,OH)$. In the same sample 5717, the amblygonite group minerals may display in addition to tavorite-montebrasite also a relatively high amblygonite component. The composition of the brownish amblygonite group mineral found in sample 5708 (Tab. 2a) corresponds to the formula $Li(Al,Fe)(PO_4)(OH)$. In this sample, the substitution of Al^{3+} by Fe^{3+} and F contents below detection limit leads to a predominantly tavoritic composition, with subordinate montebrasite. The typical brownish staining is due to exsolution of the Fe component in a late metamorphic overprint and the consequent formation of very fine-grained iron oxides or hydroxides. However, the possible effect of weathering cannot be excluded.

Berlinite, $AlPO_4$, is indicated by some very small XRD peaks in rock type A3 only. However, it could be identified neither by optical microscopy nor by microprobe analysis.

Minerals of both the *goyazite/svanbergite* and *goyazite/crandallite* solid solution series are found in rock type A4, in which they form mostly brownish grains associated with lazulite in the muscovite- and quartz-rich matrix, but also brownish coronas around lazulite patches (fig. 4*b*). Such coronas of svanbergite around lazulite were described by Lacroix (1923) and by Lasnier and Fritsch (1997) from lazulite-bearing rocks at Horrsjöberg (Sweden) and Madagascar.

According to Mandarino (1999), svanbergite and woodhouseite belong to the beudantite group, general formula $AB_3(XO_4)(SO_4)(OH)_6$, in which A = Ba, Ca, REE, Pb, Sr, (H_3O); B = Al, Fe^{3+}, and X = As, P. Minerals of this group are isostructural with the alunite mineral series and are presumed to exhibit solid solution, not only within, but also between the series (Wise, 1975; Stoffregen and Alpers, 1987).

Again according to Mandarino (1999), goyazite and crandallite belong to the crandallite group, general formula $AB_3(XO_4)_2(OH,F)_6$, in which A = Ba, Bi, Ca, REE, Pb, Sr, Th; B = Al, Fe^{3+}, and X = As, P, Si. Microprobe mineral analyses show minor La and Ce contents, indicating substitution in the A site, whereas the B site is occupied only by Al.

The compositional data in the quaternary system woodhouseite-svanbergite goyazite-crandallite, plotted in fig. 6, confirms the existence of a solid solution series between svanbergite and goyazite and between goyazite and crandallite. This supports the existence of a solid solution series between the beudantite and crandallite groups, as already hypothesized by Wise (1975) and Morteani and Ackermand (1996).

Tourmaline is a quite common constituent of rock types A3 and A4. It shows weak zoning with a dark green rounded core and a light green euhedral rim, and sometimes forms garben-like aggregates. The tourmaline core is enriched in Fe compared with the rim (Table 2*b*). This change in chemical composition follows the substitution Mg ⇔ Fe. Na content is remarkably low, due to an alkali-site deficiency, which classifies this tourmaline as Mg- to Fe-foitite depending on the Fe to Mg ratio (MacDonald *et al.*, 1993; Hawthorne and Henry, 1999). Alkali-deficient tourmaline is considered to be typical of Al- and B-rich lithologies such as tourmaline and dumortierite (Foit, 1989; Foit *et al.* 1989).

Dumortierite is rarely found as small euhedral needles, often included in kyanite in rock type B (fig. 4*d*). This rock type is characterized by the absence of phosphates and very low P contents in the whole-rock composition. Dumortierite was never found in rock type A, although the whole-rock has boron contents of up to 2670 ppm (e. g. sample 5722, Table 1). Its chemical composition is listed in Table 3.

Kyanite may form up to 20 vol% in rock types A1, A2 and B. It mostly occurs as euhedral to subhedral grains and is typically associated with coarse-grained muscovite and

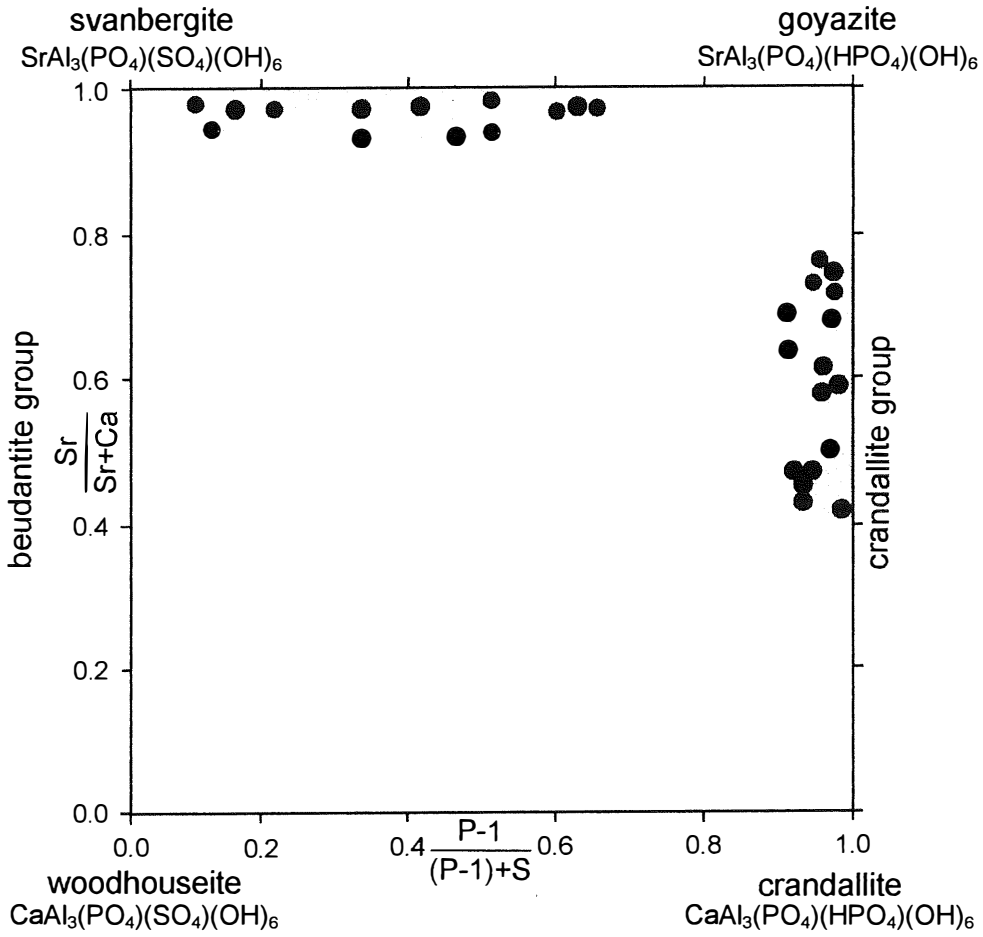

Fig. 6 – Composition of Al-phosphates as found in rock type A4, plotted in four-component system svanbergite-goyazite-woodhouseite-crandallite.

quartz. Its chemical composition is shown in Tables 2b and 3.

Andalusite is found only in rock type A1 as typical large anhedral blasts overgrowing rather fine-grained anhedral lazulite and muscovite. The chemical composition of andalusite is very similar to that of kyanite, as given in Table 2b. Some A1 rock type samples contain up to 30 vol% of andalusite. Inclusions of small kyanite grains in the rim of andalusite are very rare.

Muscovite is present at least in two generations in all rock types. The older generation is very fine-grained and produces prominent schistosity. Muscovite is often intimately intergrown as symplectite with lazulite, quartz and svanbergite. The younger generation forms elongated laths and is often closely associated with large but mainly corroded kyanite.

The main difference between fine- and coarse-grained muscovite is the K_2O content.

The fine-grained type has a low K_2O content, down to 5 wt%, whereas the coarse-grained version is around 10 wt%. As the sampling area is subtropical with deep lateritic weathering, low K_2O contents may be due to alkali loss by incipient weathering of fine-grained muscovite.

Pyrophyllite, determined by microprobe and XRD only, forms in some of the samples as very fine-grained thin rims around kyanite and andalusite.

Ti-bearing hematite is present in all studied rock types. Microprobe data show a rather strong scatter in the Fe-Ti ratios. TiO_2 contents of hematite in rock type A1 range from 0.2 to 0.6 wt%, in A2 between 0.7 and 1.3 wt%, in A3 from 1.0 to 5.0 wt%, and in A4 from 0.8 to 1.0 wt%. In rock type B, TiO_2 contents in Ti-bearing hematite are very homogeneous between 0.5 and 0.7 wt%. Neither microprobe data nor reflected light microscopical investigations showed exsolution or zoning.

Quartz forms the fine-grained groundmass and also coarse-grained polycrystalline elongated aggregates. The latter may be interpreted as pebbles of a tectonically deformed metaconglomerate. The differing amounts and distributions of opaque minerals indicate that the quartz pebbles originate from very different but prevailing metasedimentary sources. Polygonal quartz grain boundaries indicate strong static post-deformational annealing with recrystallisation.

Discussion and conclusions

Stability of Al-phosphates and -borates

Thin-section studies indicate that lazulite probably started to grow early in the metamorphic and deformational history of the rocks, when they were already intensely foliated and folded but had a very fine grain size. The well-preserved fine-grained inclusions of opaque minerals in the core of lazulite blasts demonstrate that the already crystallized lazulite behaved as a refractory mineral in subsequent metamorphic events. Lazulite rims surrounding the old cores show not only a darker blue colour but also contain coarse opaque inclusions. The sigmoidal distribution of these coarse-grained opaque inclusions indicates that the lazulite rims crystallized syn- to post-tectonically. The temperature estimate of about 460°C given by the stable oxygen isotope composition on quartz and hematite, should be close to the maximum temperature of the last metamorphic event of Brasiliano age (fig. 7). The prevalently post-tectonic lazulite is the deep blue anhedral rounded type, which can be found in crystals of up to 5 cm in diameter in only slightly deformed quartz veins discordantly cutting any schistosity.

Rims of lazulite around augelite indicate the formation of lazulite at the expense of augelite (fig. 4*a*), the first occurrence of which in metamorphic rocks was reported by Hoffmann (1979). The observation that lazulite aggregates are often surrounded by a fine-grained svanbergite rim suggests breakdown of lazulite to svanbergite (fig. 4*b*). Both reactions are the result of increasing metamorphic conditions.

Kyanite is the typical aluminium silicate in the metaquartzite. Andalusite occurs rarely. The age relations between andalusite and kyanite are equivocal, but kyanite is probably younger than andalusite, in spite of the fact that small kyanite grains are sometimes found included in andalusite. Early growth of andalusite in a still fine-grained rock is supported by the fact that lazulite and muscovite included in andalusite are typically fine-grained. Pyrophyllite rims around kyanite and andalusite should be considered as products of late low-temperature retrograde metamorphism.

Dumortierite needles were only found in one rock specimen (fig. 4*d*). With respect to the data given by Chopin *et al.* (1995), the studied dumortierite is very poor in Mg, indicating not particularly high pressure. At moderate pressures of 3 to 4 kbar the upper stability limit of dumortierite is given by Werding and

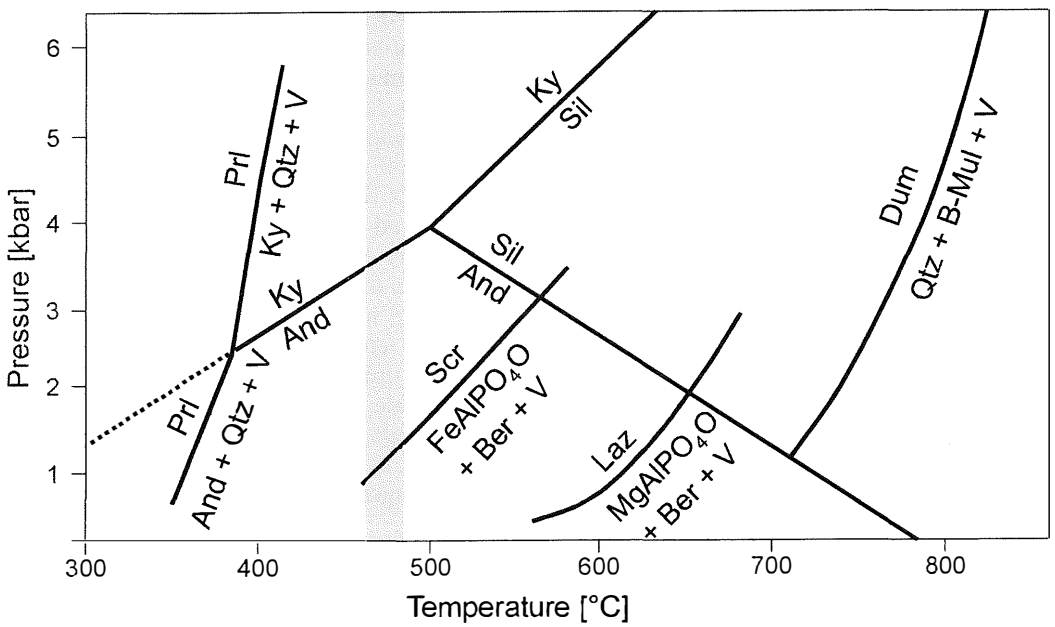

Fig. 7 – P,T-stability diagram of aluminium silicates, pyrophyllite, scorzalite and lazulite (Schmid-Beurmann, 1997) and dumortierite (Werding and Schreyer, 1996). Grey shading: temperature as deduced from stable oxygen isotope data on quartz and hematite. And: Andalusite, Ky: kyanite, Prl: pyrophyllite, Qtz: quartz, Sil: sillimanite, Scr: scorzalite, Laz: lazulite, Ber: berlinite, Dum: dumortierite.

Schreyer (1996) as about 700°C, well above the triple point of Al_2SiO_5 polymorphs (fig. 7).

Detailed data on the age and P,T conditions of the two metamorphic events for the Banderinha formation have not been published. The maximum P,T conditions of about 440°C and at least 3.5 kbar for the second and highest metamorphic stage, as shown in fig. 7, are well within the stability fields of andalusite, kyanite, dumortierite, scorzalite and lazulite (Werding and Schreyer, 1996; Cemić and Schmid-Beurmann, 1997; Schmid-Beurmann, 1997; Schmid-Beurmann *et al.*, 1997).

Stratigraphic and tectonic position

As discussed above, there are good reasons for using phosphate-bearing lithologies as the basis of the Banderinha formation. Nevertheless, if the lithologies and mineral parageneses given, for example by Almeida Abreu (1996), are taken as representative, phosphate-bearing lithologies fit much better into the Barão de Guacúi than the Banderinha formation. In fact, the description of the Barão de Guacúi formation, *i.e.* muscovite schists with quartz, kyanite and tourmaline, quartzschists and metaquartzites, is almost perfect for phosphate-bearing rocks, whereas that of the Banderinha formation (meta-arenites, in many cases red beds, with local metaconglomerates) is not very appropriate.

In any case, phosphate-bearing rocks represent an important border dividing the Costa Sena and Guinda groups (fig. 2) i.e. between the Rio Paraúna and Espinhaço supergroups, which is otherwise difficult to recognize due to a detachment fault which extensively tectonised the erosive contact (Almeida Abreu, 1994, 1996; Horn *et al.*, 1996).

Protolith and depositional environment

The chemical composition of the lazulite-bearing muscovite-kyanite metaquartzites is characterised by high aluminium, phosphorus, fluorine and boron, and low calcium and sodium contents. From the texture of opaque minerals included in the cores of lazulite, the protolith was very fine-grained.

The evolution of the Middle Proterozoic Espinhaço rift started around 1700 Ma ago with extension and crustal thinning, followed by invasion of the sea into the rift system (Dussin, 1994; Horn *et al.*, 1996). The deposition of the phosphate- and borate-bearing metaquartzitic sediments of the Banderinha formation took place at this stage in a shallow-water facies. The sea entering the Espinhaço rift was part of the early oceans which were probably «soda oceans», rich in silica and ferrous iron but relatively poor in calcium and magnesium and generally devoid of sulphate due to the lack of oxygen (Einsele, 1992). Nevertheless, due to the appearance of the first stromatolites and the resulting onset of photosynthesis in the Upper Archean, organic life was locally possible, with consequent sedimentation of phosphate-bearing subtidal, intertidal or supratidal series (Song and Gao, 1985; Einsele, 1992). If marine sediments are suggested as the protolith, then the low Na content of phosphate-bearing rocks needs explanation. But if a sabkha-like coastal environment is presumed, then fresh-water flash floods were able to reduce the Na content stored in the sediments by dissolving highly soluble Na salts, halite and/or soda. Relatively insoluble phosphates, as well as B and Li, were left in place and bound to clay minerals. During the Brasiliano tectonothermal event between 680 and 450 Ma ago, these elements contributed to the formation of various phosphates and of dumortierite and amblygonite.

The second possible type of environment was a closed lake system in a semi-arid to arid climate (Einsele, 1992). K, P, B and Li may have accumulated in the lake sediments and, as in the previous model, flash floods supplied coarse-grained clastic sediments and selectively dissolved highly soluble salts such as halite and soda. Both situations fit the general picture of the development of the Espinhaço rift as given by Dussin (1994).

The third possible alternative, discussed by Schreyer (1987) and Morteani and Ackermand (1996), is a volcanic protolith of acidic composition with sericitic alteration due to permeation with magmatic fluids. In the course of such a process, Ca and Na were selectively depleted, and Si, Al, P, Li and B were relatively enriched.

Marine deposition process seems to be the most probable process. It is supported by the fact that even in Archean rocks Sr, Fe, Al, Ca and REE phosphates may be minor components of marine sediments (Rasmussen, 1996). The protolith acquired its present–day mineral composition and texture during the Brasiliano event.

ACKNOWLEDGMENTS

The Deutsche Forschungsgemeinschaft supported research with grant Mo-232/26-3. The authors also thank Ch. Chopin (Paris), E. Libowitzky and M.A. Götzinger (Vienna) for their helpful comments. J.P. Cassedanne (Rio de Janeiro) and G. Knauer (Belo Horizonte) gave helpful information for field work and the «Eschwege» Research Center of Geology in Diamantina (Brazil) supplied a car with driver. Mrs. B. Mader (Kiel) helped with microprobe analyses and A. Gilg (München) determined stable oxygen isotopes.

REFERENCES

ALMEIDA ABREU P.B., PFLUG R. and SCHORSCHER H.D. (1992) — *Cover/Basement relationships in the southern Serra do Espinhaço, Minas Gerais, Brazil*. Zbl. Geol. Paleont., **1**, 1749-1760.

ALMEIDA ABREU P.A. (1994) — *A evolução geochimica da Serra do Espinhaço Meridonal, Minas Gerais, Brazil*. Ph. D. thesis, Albert-Ludwigs-Universität Freiburg, 150 p.

ALMEIDA ABREU P.A. (1996) — *O caminho das pedras*. Geonomos, **4**, 77-93.

BANK H. (1972) — *Blauer und dunkelgrüner durchsichtiger Lazulith aus Brasilien*. Zt. Dtsch. Gemmol. Ges., **21**, 219-221.

BOTTINGA Y. and JAVOY M. (1973) — *Comments on oxygen isotope geothermometry.* Earth Planet. Sci. Lett., **20**, 250-265.

CASSEDANNE J.P. (1990) — *Un nouveau matériaux gemme: Le metaquartzite à lazulite (Bahia-Brésil).* Revue de Gemmologie, **105**, 16-18.

CASSEDANNE J.P. and FRANCO R.R. (1966) — *Indices de dumortiérite de la Serra de Vereda (Municipes de Macaubas et Boquira, Etat de Bahia).* Anais Acad. Bras. Ciências, **38**, 47-52.

CASSEDANNE J.P. and CASSEDANNE J.O. (1975) — *Note sur la lazulite de la région de Diamantina (MG).* An. Acad. Bras. Cienc., **47**, 283-288.

CASSEDANNE J.P., CASSEDANNE J.O. and CARVALHO H.F. (1989) — *Origine des lazulites liées à des accidents ferrifères dans des métaquartzites à dumortierite (Serra de Vereda, Bahia, Brésil).* An. Acad. Bras. Cienc., **61**, 59-72.

CEMIĆ L. and SCHMID-BEURMANN P. (1997) — *Lazulite stability relations in the system* Al_2O_3 - $AlPO_4$ - $Mg_3(PO_4)_2$ - H_2O. Mineral. and Petrol., **61**, 211-222.

CHIBA H., CHACKO T., CLAYTON R. N. and GOLDSMITH, J.R. (1989) — *Oxygen isotope fractionations involving diopside, forsterite, magnetite and calcite: applications to geothermometry.* Geochim. Cosmochim. Acta, **53**, 2985-2995.

CHOPIN C., FERRARIS G., IVALDI G., SCHERTL H.-P., SCHREYER W., COMPAGNONI R., DAVIDSON, C. and DAVIS, A.M. (1995) — *Magnesiodumortierite, a new mineral from very-high-pressure rocks (western Alps). II: Crystal chemistry and petrological significance.* Eur. J. Mineral., **7**, 525-535.

CLAYTON R. and MAYEDA T.K. (1963) — *The use of bromine pentafluoride in the extraction of oxygen from oxides and silicates for isotope analysis.* Geochim.Cosmochim. Acta, **27**, 43-52.

DORR J.V.N. (1969) — *Physiographic, stratigraphic and structural development of the Quadrilatero Ferrifero, Minas Gerais, Brazil.* U.S. Geolog. Surv. Pap., **641-A**, 4-15.

DUSSIN I.A. (1994) — *Evolution structurale de la region de l'Espinhaço Meridional, Bordure Sud-Est du Craton São Francisco, Brésil.* PhD. thesis, Université d'Orléans, 260 p.

EBERLE W. (1972) — *Petrographische und geologische Untersuchungen in der Umgebung von Diamantina (Espinhaço-Zone, Minas Gerais, Brasilien).* Beih. Geol. Jb., **121**, 5-58.

EINSELE G. (1992) — *Sedimentary basins: Evolution, facies and sediment budget.* Springer Verlag, Berlin, 628 p.

FOGAÇA A.A.C. and SCHÖLL W.U. (1984) - *Estratigrafia e tectonica das rochas Arqueanas e Proterozoicas da região de Guinda e Gouveia (MG).* Anais XXXIII Congr. Bras. Geol. An., 2639-2653.

FOIT F.F. (1989) — *Crystal chemistry of alkali-deficient schorl and tourmaline structural relationships.* Am. Min., **74**, 422-431.

FOIT F.F., FUCHS Y. and MYERS P.E. (1989) — *Chemistry of alkali-deficient schorls from two tourmaline-dumortierite deposits.* Am. Min., **74**, 1317-1324.

HAWTHORNE F.C. and HENRY D.J. (1999) — *Classification of the minerals of the tourmaline group.* Eur. J. Mineral, **11**, 201-215

HERRGESELL G. and PFLUG R. (1986) — *The thrust belt of the southern Serra do Espinhaço, Minas Gerais, Brazil.* Zbl. Geol. Paleont., **1985**, 1405-1414.

HOFFMANN C. (1979) — *Augelite, a rare aluminium phosphate: First find in a metamorphic environment.* N. Jb. Miner. Abh., **136**, 1-9.

HORN A., MORTEANI G. and ACKERMAND D. (1996) — *Significância da ocorrência de fosfatos e boratos de alumínio no contato entre os supergrupos Rio Paraúna e Espinhaço na região de Diamantina, Minas Gerais, Brasil.* Geonômos, **4**, 1-10.

LACROIX A. (1923) — *Minéralogie de Madagascar.* 3 Vols., ed. Challamel, Paris.

LASNIER B. and FRITSCH E. (1997) — *About a blue quartz from Madagascar.* 26th Int. Gemm. Conf., Abstr., 33-34.

MACDONALD D.J., HAWTHORNE F.C. and GRICE J.D. (1993) — *Foitite,* $\square[Fe_2^{2+}(Al,Fe^{3+})]Al_6Si_6O_{18}(BO_3)_3(OH)_4$, *a new alkali-deficient tourmaline: Description and crystal structure.* Am. Min., **78**, 1299-1303.

MANDARINO J.A. (1999) — *Fleischer's Glossary of mineral species.* The Mineralogical Record Inc., 8th ed., Tucson, 225 p.

MCLENNAN S. M. (1989) — *Rare earth elements in sedimentary rocks: Influence of provenance and sedimentary processes.* In: «Geochemistry and Mineralogy of Rare Earth Elements» B.R. LIPIN and G.A. MCKAY, (Eds.), Reviews in Mineralogy -, **21**, Mineral. Soc. Am., Washington D.C., 169-200.

MORTEANI G. and ACKERMAND D. (1996) — *Aluminium phosphates in muscovite kyanite metaquartzites from Passo di Vizze (Alto Adige, NE Italy).* Eur. J. Mineral., **8**, 1-17.

PFLUG R. (1965) — *A geologia da parte meridional da Serra do Espinhaço e zonas adjacentes, Minas Gerais.* DNPM, Div. Geol, Min. Bol., **226**, 1-55.

PFLUG R. (1968) — *Observações sobre a estratigrafia da Serie Minas na região de Diamantina, Minas Gerais.* DNPM, Div. Geol. Min. Notas Prelim. Estud., **142**, 1-20.

PFLUG R. and CARVALHO R.T. (1964) — *A evolução estrutural da região de Gouveia, Serra do Espinhaço, Minas Gerais.* DNPM, Div. Geol. Min., **213**, 1-37.

PFLUG R., HOPPE A. and BRICHTA A. (1980) — *Paleogeografia do Precambriano na Serra do Espinhaço, Minas Gerais, Brasil.* Nuevos Resultados Pesquisa Alemana Latinoam., DFG, Boppard, 33-34.

POUCHOU J.L. and PICHOIR F. (1984) — *A new model for the quantitative X-ray microanalysis. Part I: Application to the analysis of homogeneous samples.* La Recherche Aérospatiale, **3**, 12-36.

RASMUSSEN B. (1996) — *Early-diagenetic REE-phosphate minerals (florencite, gorceixite, crandallite, and xenotime) in marine sandstones: A major sink for oceanic phosphorus.* Am. J. Sci., **296**, 601-632

SCHMID-BEURMANN P. (1997) — *Phosjha-mineralogie und ihre experimentellen materialwissenschaftlichen Aspekte dargestellt am Beispiel des Lazulith-Typs.* Habilitationsschrift, Christian-Albrechts-Universität Kiel, 153 p.

SCHMID-BEURMANN P., MORTEANI G. and CEMIĆ L. (1997) — *Experimental determination of the upper stability of scorzalite, $FeAl_2[OH/PO_4]_2$, and the occurrence of minerals with a composition intermediate between scorzalite and lazulite (ss) up to conditions of the amphibolite facies.* Mineral. Petrol., **61**, 211-222.

SCHÖLL W.U. and FOGAÇA A.C.C. (1979) — *Estratigrafia da Serra do Espinhaço na região de Diamantina (M.G.).* Anais Simpos. Geol. Minas Gerais, Diamantina, 55-73.

SCHÖLL W.U. and FOGAÇA A.C.C. (1981) — *Mapeamento geologico das quadriculas Guinda e Gouveia (MG).* Projeto Mapeamento Espinhaço, DNPM/CPRM, 1-51.

SCHREYER W. (1987) — *Pre- or synmetamorphic metasomatism in peraluminous metamorphic rocks.* In: *«Chemical Transport in Metasomatic Processes»* H.C. HELGESON, (Ed.), 265-296.

SILVA R.R. (1995) — *Contribution to the stratigraphy and paleogeography of the Lower Espinhaço supergroup (Mesoproterozoic) between Diamantina and Gouveia, Minas Gerais, Brazil.* Ph. D. Thesis, Universität Freiburg, 275 p..

SÖLLNER F., LAMMERER B. and WEBER-DIEFENBACH K. (1991) — *Die Krustenentwicklung in der Küstenregion nördlich von Rio de Janeiro/Brasilien - Altersbestimmungen (U/Pb an Zirkon und Rb/Sr an Gesteinen) an hochdruck- und temperaturfaziellen Gesteinen des Ribeira Mobile Belt und des São Francisco Kratons (Espirito Santo/Minas Gerais).* Münchener Geologische Hefte, **3**, 100 p.

SONG T. and GAO J. (1985) — *Tidal sedimentary structures from the Upper Precambrian rocks of the Ming tombs district, Beijing (Peking), China.* Precamb. Res., **29**, 93-107.

STOFFREGEN R.E. and ALPERS C.N. (1987) — *Woodhouseite and svanbergite in hydrothermal ore deposits: Products of apatite destruction during advanced argillic alteration.* Can. Mineral., **25**, 201-211.

WERDING G. and SCHREYER W. (1996) — *Experimental studies on borosilicates and selected borates.* In: «Boron Mineralogy, Petrology and Geochemistry» E.S. GREW and L.M. ANOVITZ, Eds., Reviews in Mineralogy, **33**, Mineral. Soc. Am., Washington D.C, 117-163.

WISE W.S. (1975) — *Solid solution between the alunite, woodhouseite and crandallite mineral series.* N. Jb. Miner. Mh., **12**, 540-545.

ZHENG Y.-F. and SIMON K. (1991) — *Oxygen isotope fractionation in hematite and magnetite: A theoretical calculation and application to geothermometry of metamorphic iron-formations.* Eur. J. Mineral., **3**, 877-886.